Single-photon double ionization of helium in presence of DC electric field.

I. A. Ivanov*† and A. S. Kheifets

Research School of Physical Sciences and Engineering,

The Australian National University, Canberra ACT 0200, Australia

(Dated: August 25, 2006)

Abstract

We study the influence of the external DC electric field on the process of single-photon double ionization of helium at photon energies of 85 and 90 eV. Calculation is based on a numerical solution of the time-dependent Schrödinger equation and subsequent projection of the solution on a final state furnished by the convergent close coupling (CCC) expansion. We find that for the range of the field strengths studied ($F_{\rm DC} \leq 3 \times 10^{-2}$ a.u.) the presence of the external DC field leads to a monotonous decrease of the total probability of single-photon double electron ionization. This decrease is achieved primarily due to decreasing probability to detect electrons with unequal energy sharing.

* Corresponding author: Igor.Ivanov@.anu.edu.au

† On leave from the Institute of Spectroscopy, Russian Academy of Sciences

I. INTRODUCTION

Single-photon double ionization of helium has been studied extensively over the past decade across a wide range of photon energies from meV [1] to keV [2] regimes. Basic mechanisms of this process are now well understood, both qualitatively and quantitatively, with accurate theoretical predictions being confirmed experimentally under a wide range of kinematical conditions [3–5]. The emphasis in double photoionization (DPI) studies is now shifting towards the multi-photon processes in stronger electromagnetic fields [6] or/and more complex atomic [7, 8] and molecular [9, 10] targets where electron correlation may play a more prominent role. In the present work, we introduce another factor which may complicate single-photon double ionization, a static electric field. We consider the DPI of helium subjected to an external DC field with the strength ranging from few hundreds to few tens of the atomic unit.

The motivation of this study is two-fold. First, we want to examine the correlated many-body dynamics of two-electron escape under the influence of the static electric field. Since the pioneering work of Wannier [11], it is well known that the double ionization is a "balancing act" between the inter-electron repulsion and the nucleus drag with only very few selected trajectories leading to the two-electron escape. The static field may upset this delicate balance or open up new possible two-electron escape routes. This can result in a net decrease or increase of the DPI cross-section and changing energy and angular distribution of the photoelectron pair.

On a more pragmatic level, we want to test a new computational procedure aiming to describe two-electron ionization processes in atoms subjected to short pulses of electromagnetic and/or static electric fields. The presence of a static electric field opens up a new, tunneling ionization mechanism which cannot be described within the perturbation theory (PT) even in the weak field regime. So the theoretical treatment should be non-perturbative.

Our method is based upon numerical integration of the time-dependent Schrödinger equation (TDSE) by expanding the solution on a suitable square integrable basis. Similar time-dependent methods have been used extensively in strong field ionization studies of two-electron atomic targets with variety of bases employed, e.g. explicitly correlated [12],

multiconfiguration Hartree-Fock [13] and Coulomb wavepackets [14]. In our implementation of the TDSE method, we construct a two-electron basis from the pseudostates obtained by diagonalizing the He^+ Hamiltonian on a Laguerre basis [15]. Once the solution of the TDSE is found, various cross-sections can be obtained by projecting the TDSE wave function on a set of the field-free final states of the helium atom with both electrons in continuum. Proper description of such states is, by itself, a rather complicated problem. There has been various methods proposed to solve this problem. One can incorporate the correct boundary conditions needed to describe two electrons in continuum using the exterior complex scaling method [16–18]. The problem of imposing correct boundary conditions can be avoided altogether with the help of the procedure using the complex Sturmian basis [19]. Hyperspherical R-matrix method with the semiclassical outgoing waves was used to represent the final double continuum state in the problem of double ionization of helium [20]. One can also use approaches based on the various implementations of the close-coupling method [15, 21–23]. In the present work, we use the so-called convergent close-coupling (CCC) expansion to describe the field-free two-electron continuum. This provides a far more accurate description of the inter-electron correlations as compared with a finite order PT employed by other authors [24, 25].

To the best knowledge of the authors, the present work is the first study of the effect of the static DC field on DPI of He. There have been previous reports on the DC field effect on double photoexcitation of helium [26–28]. Because of a large radial extent of the highly excited Rydberg states involved in these studies, much weaker DC fields were needed to observe a noticeable effect. In the present study, the static field is competing with the nucleus field at smaller distances which requires a much stronger DC field strength.

The paper is organized as follows. In Sec. II we outline the theoretical procedure. In Sec. III we give numerical details and assess the accuracy of our computational procedure. In Sec. IV we discuss the results. Finally, we conclude by discussing application of the present method to other processes and atomic targets.

II. THEORY.

We seek a solution of the TDSE for the helium atom

$$i\frac{\partial\Psi}{\partial t} = \hat{H}\Psi, \tag{1}$$

with the Hamiltonian

$$\hat{H} = \hat{H}_0 + \hat{V}_{12} + \hat{H}_{\rm int}(t), \tag{2}$$

where the non-interacting Hamiltonian and the Coulomb interaction are, respectively,

$$\hat{H}_0 = \frac{\boldsymbol{p}_1^2}{2} + \frac{\boldsymbol{p}_2^2}{2} - \frac{2}{r_1} - \frac{2}{r_2}, \tag{3}$$

$$\hat{V}_{12} = \frac{1}{|\boldsymbol{r}_1 - \boldsymbol{r}_2|}\ . \tag{4}$$

The interaction with the external electromagnetic and static fields is written in the length gauge:

$$\hat{H}_{\rm int}(t) = f(t)(\boldsymbol{r}_1 + \boldsymbol{r}_2)\cdot(\boldsymbol{F}_{\rm AC}\cos\omega t + \boldsymbol{F}_{\rm DC}), \tag{5}$$

Here $f(t)$ is a smooth switching function the detailed form of which will be given below. The AC electric field is assumed to be linearly polarized. For the sake of simplicity, we chose the AC and DC fields to be parallel and employ the same switching function for both fields.

The solution of the TDSE is sought in the form of expansion on a square-integrable basis

$$\Psi(\boldsymbol{r}_1, \boldsymbol{r}_2, t) = \sum_j a_j(t) f_j(\boldsymbol{r}_1, \boldsymbol{r}_2). \tag{6}$$

Here

$$f_j(\boldsymbol{r}_1, \boldsymbol{r}_2) = \phi^N_{n_1 l_1}(r_1)\phi^N_{n_2 l_2}(r_2)\ |l_1(1)l_2(2)\ L\rangle, \tag{7}$$

where notation $|l_1(1)l_2(2)\ L\rangle$ is used to represent two spherical functions coupled in a standard way to a state with the total angular momentum L by means of the Clebsch-Gordan coefficients: $|l_1(1)l_2(2)\ L\rangle = \sum_{m_1 m_2}(l_1 m_1 l_2 m_2|LM)Y_{l_1 m_1}(\boldsymbol{n}_1)Y_{l_2 m_2}(\boldsymbol{n}_2)$. Index j is used as a shortcut for the set of quantum numbers n_1, l_1, n_2, l_2, L specifying a basis vector. The radial orbitals in Eq. (7) are pseudostates obtained by diagonalizing the He^+ Hamiltonian in a Laguerre basis [15]:

$$\langle\phi^N_{nl}|\hat{H}_{\rm He^+}|\phi^N_{n'l'}\rangle = E_i\delta_{nn'}\delta_{ll'}\ .$$

Here E_i is the energy of a pseudostate and N is the size of the basis.

The pseudostates with positive energies provide a square integrable representation of the continuous spectrum [23]. In the present work, this feature of the pseudostates is exploited in a two-fold manner. First, we use the pseudostates for the construction of the basis set Eq. (7). Thus constructed basis set is orthogonal and diagonalizes the non-interacting Hamiltonian $\langle i|\hat{H}_0|j\rangle = \delta_{ij}\lambda_i$, where λ_i is a sum of corresponding pseudostate energies. Specific details about this procedure will be given below. Second, we employ the pseudostates (not necessarily the same set) within the CCC formalism to construct the two-electron field-free final states representing various ionization channels.

After the set of the basis functions (7) is chosen, we can rewrite the TDSE as a set of ordinary differential equations for the components $a_j(t)$:

$$i\dot{a}_k - \lambda_k a_k = \sum_j \langle k|\hat{V}_{12} + \hat{H}_{\rm int}|j\rangle a_j, \tag{8}$$

To impose the initial condition for the set of equations (8), we perform a separate diagonalization of the field-free Hamiltonian on the same basis. We assume that at the moment $t = 0$ the atom is in its ground state and find the vector $\boldsymbol{a}(0)$.

We integrate Eq. (8) up to a time T_1 when the external fields are switched off. Then we project the solution of Eq. (8) onto a field-free CCC basis. Thus, the probabilities to find the helium atom in any specific field-free state can be computed including the doubly ionized states which are of particular interest to us in the present work.

In the CCC formalism, the interacting two-electron state is represented by a close-coupling expansion over the channel states each of which is composed of a target pseudostate f and a Coulomb wave $\boldsymbol{k}$:

$$\Psi_f(\boldsymbol{k}) = |\boldsymbol{k}f\rangle + \sum_{\boldsymbol{k}'j} \frac{\langle \boldsymbol{k}f|T|\boldsymbol{k}'j\rangle}{E - k'^2/2 - \varepsilon_j + i0}|\boldsymbol{k}'j\rangle \tag{9}$$

Here $\langle \boldsymbol{k}f|T|\boldsymbol{k}'j\rangle$ is half-on-shell T-matrix which is found by solving a set of coupled Lippmann-Schwinger equations. [23]. It is convenient to strip wave function (9) of its angular dependence using a partial wave decomposition:

$$\Psi_f(\boldsymbol{k}) = \sum_{\substack{lm\\JM}} \Psi_{lf(J)}(k)\langle lml_f m_f|JM\rangle Y_{lm}(\hat{\boldsymbol{k}}), \tag{10}$$

where $\langle lml_f m_f | JM \rangle$ are the Clebsch-Gordan coefficients. The two-electron wave-function $\Psi_{lf(J)}(k)$ is defined in terms of the reduced matrix elements of the T-matrix as:

$$\Psi_{lf(J)}(k) \equiv \|kl\, n_f l_f; J\rangle + \sum_{jl'} \!\!\!\!\!\!\int k'^2 dk' \frac{\langle kl\, n_f l_f \| T_J \| n_j l_j k' l'; J\rangle}{E - k'^2/2 - \varepsilon_j + i0}\, \|k' l'\, n_j l_j\rangle, \qquad (11)$$

where $\|kl\, n_f l_f; J\rangle$ is a product of a Coulomb wave function kl and a pseudostate $n_f l_f$ coupled to a total angular momentum J.

The CCC wave functions (9)–(11) are written as a solution of a scattering problem with the index f referring to a bound state of the target hydrogen-like ion (He^+ in the present case). However, if we choose a target pseudostate f of some positive energy E_f, then the CCC wave functions $\Psi_{lf(J)}(k)$ can be used to construct a wave function of the state with two electrons in the continuum:

$$\Psi(\boldsymbol{k}_1, \boldsymbol{k}_2) = \sum_{\substack{l_1 m_1 \\ l_2 m_2}}^{J,M} \langle l_1 m_1 l_2 m_2 | JM \rangle Y_{l_1 m_1}(\hat{\boldsymbol{k}}_1) Y_{l_2 m_2}(\hat{\boldsymbol{k}}_2) e^{i[\delta_{l_f}(k_2) + \delta_{l_1}(k_1)]} \Psi_{l_1 f(J)}(k_1) \langle k_2 l_2 \| n_f l_f \rangle \ . \qquad (12)$$

Here $\delta_{l_1}(k_1)$ and $\delta_{l_f}(k_2)$ are the Coulomb phases with $Z_1 = 1$ and $Z_2 = 2$ respectively, and $\langle k_2 l_f \| n_f l_f \rangle$ is an overlap of the pseudostate and the Coulomb wave function with the same energy $E_f = k_2^2/2$ and the angular momenta $l_2 = l_f$. This recipe of constructing the state with two electrons in continuum has been applied for calculations of DPI of helium-like targets in earlier works [29, 30].

III. NUMERICAL DETAILS

A. Solution of TDSE

In the present work, we consider modestly strong electric fields: the AC field of the order of 0.1 a.u. corresponding to 3.5×10^{14} W/cm^2 intensity, and the DC field not exceeding 0.03 a.u. This allows us to retain terms with total angular momentum $J = 0 - 2$ in expansion (6). To represent each total angular momentum block, we proceed as follows. For all S, P, D total angular momentum states we let l_1, l_2 vary within the limits $0 - 3$. The total number of pseudostates participating in building the basis states was 20 for each l. To represent $J = 0, 1, 2$ singlet states in expansion (6), we used all possible combinations of

these pseudostates. Such a choice gave us 840 basis states of S-symmetry, 1200 basis states of P-symmetry and 1430 states of D-symmetry, resulting in a total dimension of the basis equal to 3470.

To check convergence of the basis, we performed a separate calculation in which we added a subset of 20 pseudostates with $l = 4$. To represent $J = 0, 1$ states in expansion (6), we used all possible combinations of the enlarged set of the pseudostates. To represent $J = 2$ states we used only pseudostates satisfying the condition $l_1 + l_2 = 2$. This choice was motivated primarily by the desire to keep the size of the calculation manageable. Such a choice gave us 1050 basis states of S-symmetry, 1600 basis states of P-symmetry and 610 states of D-symmetry, resulting in a total dimension of the basis (6) equal to 3260. We found that with the use of this modified basis set for the solution of the TDSE, the ionization probabilities varied typically by an order of one percent.

As noted above, the initial conditions for the system of equations (8) are determined by solving a separate eigenvalue problem using a subset of basis functions of the S-symmetry. This produced the ground state energy of -2.90330 a.u. as compared with the "near exact" ground state energy of -2.90372 [31].

The switching function in the Hamiltonian (5) was chosen in such a way that the amplitudes of the fields remained constant during the time interval $(T, 4T)$, where $T = 2\pi/\omega$ was a period of the AC electromagnetic field. The fields were ramped on and off smoothly over one AC field period. The total duration of the atom-field interaction was therefore $T_1 = 6T$.

The set of ordinary differential equations (8) was solved on an interval $(0, T_1)$ with the use of the Runge-Kutta method subject to the initial condition at $t = 0$.

B. Projection on final CCC states.

In the present study, we are concerned with the process of single-photon DPI of helium. Accordingly, the final states of a field-free atom should correspond to doubly ionized states of helium lying in the P-continuum. Such states were constructed as prescribed by Eq. (12) with $J = 1, M = 0$. For the geometry considered in the paper (linearly polarized AC and DC fields directed along the quanization axis) M is a conserved quantity. The pseudostate

basis $n_j l_j$ in Eq. (11) was restricted to 30 states in each partial wave with $0 \leq l_j \leq 3$.

A set of the final states corresponding to various photoelectron energies E_1, E_2 was prepared. The energies E_1 and E_2 were taken to lie on a rectangular grid $E_i = 1, 2, 3, 4, 5, 6, 7, 8, 10, 13, 20, 40, 100\,\mathrm{eV}$. By projecting the solution of the TDSE on the states of this grid we were able to obtain a probability distribution function $p(\boldsymbol{k}_1, \boldsymbol{k}_2)$ of finding the helium atom in a field-free state $(\boldsymbol{k}_1, \boldsymbol{k}_2)$ at the time $t = T_1$. From this distribution function, various other relevant distributions can be deduced. By integrating over directions of the momenta $(\hat{\boldsymbol{k}}_1, \hat{\boldsymbol{k}}_2)$, one can obtain the energy distribution function $P(E_1, E_2)$ giving the probability to find electrons with energies E_1, E_2.

The DPI cross-section is related to the distribution function $p(\boldsymbol{k}_1, \boldsymbol{k}_2)$ normalized to the field intensity:

$$\sigma(\boldsymbol{k}_1, \boldsymbol{k}_2) = \frac{8\pi\omega}{c} \frac{p(\boldsymbol{k}_1, \boldsymbol{k}_2)}{W}, \tag{13}$$

where $W = 2\int_0^{T_1} F_{\mathrm{AC}}^2(t)\ dt$ and $c \approx 137$ is the speed of light in atomic units. The total integrated cross-section (TICS) is given by:

$$\sigma(\omega) = \frac{1}{2} \int \sigma(\boldsymbol{k}_1, \boldsymbol{k}_2)\ d\hat{\boldsymbol{k}}_1 d\hat{\boldsymbol{k}}_2 dk_1 dk_2, \tag{14}$$

Differential DPI cross-sections are usually defined using the explicit energy conservation which does not hold for ionization processes driven by short pulses. In this case, one has to apply a suitable "energy averaging" procedure as the one prescribed in Ref. [32]. With this procedure, the single differential cross-section (SDCS) can be defined as:

$$\frac{d\sigma(\omega)}{dE_1} = \frac{1}{2q_1 q_2\ \cos^2\alpha} \int \sigma(\boldsymbol{k}_1, k_1 \tan(\alpha)\hat{\boldsymbol{k}}_2)\ d\hat{\boldsymbol{k}}_1 d\hat{\boldsymbol{k}}_2\ k_1 dk_1, \tag{15}$$

where the momenta q_1, q_2 are defined on the energy shell: $E_1 = q_1^2/2$, $E - E_1 = q_2^2/2$ and $\tan\alpha = q_2/q_1$. The partial wave expansion (12) allows for an analytical angular integration in Eqs. (14) and (15). The k_1, k_2 integrations were performed using the Simpson rule and an interpolation procedure.

The cross-sections (14) and (15) become the customarily defined TICS and SDCS in the limit of infinite interaction time $T_1 \to \infty$. In the present paper, we consider short pulses with $T_1 = 6T$. We must therefore exercise certain caution when interpreting the present

cross-section results. The TICS given by Eq. (14) defines a quantity proportional to the total DPI probability. The SDCS defined by Eq. (15) gives an averaged characteristic of the curvature of the surface $P(E_1, E_2)$ near its intersection with the energy conservation plane $E_1 + E_2 = E$.

C. Accuracy of the method

Apart from issues related to the convergence of the basis set (7) addressed in Sec. III A, the principal limitation of the accuracy of the present method lies in the fact that the bases used for the solution of the TDSE and construction of the CCC field-free final states are different sets of functions which span different portions of the Hilbert space. Let $\hat{P}_{\rm B}$ be a projector on a subspace spanned by the CCC vectors, corresponding to a given set of the final states. To deterimine the probabiity of finding Helium atom in any of these states we compute the matrix element $\langle\Psi(t)|\hat{P}_{\rm B}|\Psi(t)\rangle$, where $\Psi(t)$ is solution of the TDSE obtained with the help of the basis used in the present work. Let $\hat{P}_{\rm A}$ be the projector on the subspace spanned by all basis vectors (7). Since this basis is finite and the projector $\hat{P}_{\rm A}$ is not a unit operator, the TDSE we actually solve is not Eq. (1) but rather $i\dfrac{\partial\Psi}{\partial t} = \hat{P}_{\rm A}\hat{H}\hat{P}_{\rm A}\Psi$. This circumstance may lead to spurious time-dependence in the computed probabilities. Indeed, for the free evolution of the Helium atom, when external fields are absent, the probabilities should be constant which is possible only if $[\hat{P}_{\rm A}(\hat{H}_0 + \hat{V}_{12})\hat{P}_{\rm A}, \hat{P}_{\rm B}] = 0$ (using the notation of Eqs. (3),(4)), an equality which is not automatically satisfied.

This can be put in a different form. Consider time-evolution of the helium atom in the absence of external fields. This evolution can be presented as a sum

$$\Psi_{\rm A}(t) = \sum c_k \exp^{-iE_k t}\,\Psi_k, \tag{16}$$

where Ψ_k and E_k are solutions of the eigenvalue problem for the field-free helium Hamiltonian in the basis (7). The eigenvectors Ψ_k are not strictly orthogonal to the CCC field-free states. The overlap of the solution of the TDSE and the CCC state will therefore contain terms $\sum c_k \exp^{-iE_k t}\langle\Psi_{\rm CCC}|\Psi_k\rangle$, which may introduce spurious beats in the probabilities unless the overlaps $\langle\Psi_{\rm CCC}|\Psi_k\rangle$ peak narrowly enough.

The error introduced by these beats may be reduced to an acceptable level if we choose a large enough basis to represent the CCC expansion. The representation we employ in the present calculation uses 30 pseudostates for each partial wave with $0 \leq l_j \leq 3$. A typical distribution of the overlaps of the P-symmetry is shown in Figure 1. The CCC wave function describes a state with both electrons having equal energies $E_1 = E_2$=20 eV.

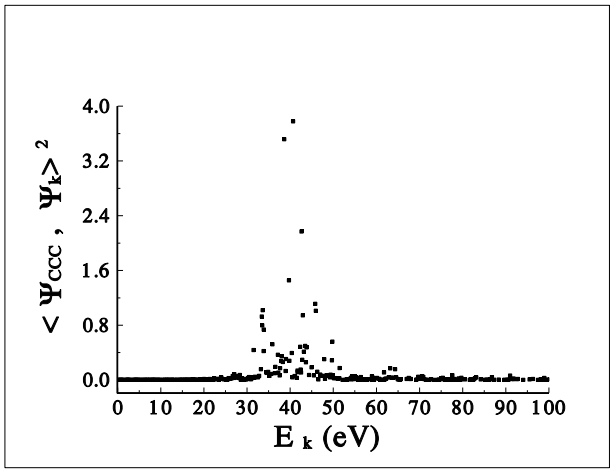

FIG. 1: Square of the overlap of the CCC wave function describing a final P-state with $E_1 = E_2 =$ 20 eV and the $P-$ symmetry eigenfunctions of for field-free helium Hamiltonian in the basis of the pseudostates (7).

TABLE I: Absolute values of the overlaps of the CCC and TDSE wave functions for different T_1.

E_1(eV)	l_1	E_2 (eV)	l_2	$\lvert\langle E_1 l_1 E_2 l_2 \rvert \text{TDSE}\rangle\rvert$	
				$T_1 = 6T$	$T_1 = 7T$
0.350	0	5.62	1	0.2544-2	0.2669-2
0.110	1	5.86	0	0.3378-2	0.3013-2
0.694	2	5.97	3	0.1102-2	0.9934-3
0.349	3	5.94	2	0.7079-3	0.4471-3
0.140	2	5.83	1	0.3436-3	0.6116-3
0.140	2	5.83	3	0.1253-2	0.1311-2

As one can see, for this CCC wave function the overlaps are narrowly peaked around the value of 40 eV. Only few of them (4 in the figure) produce significant contribution to the

sum in Eq. (16). Since the energies of these dominating states are close to each other, one can expect the beats in the cross-sections to be insignificant. This is illustrated in the Table where we present the absolute values of the overlaps of various components of the partial wave expansion (10) of the CCC wave function and the solution of the TDSE obtained for two cases. In the first calculation, the external fields are switched off and the overlaps are computed at the same time $T_1 = 6T$. In the second calculation, we let the system evolve freely after switching off external fields for the duration of one period of the AC field and compute overlaps at the time $T_1 = 7T$. As one can see from the Table, the variation in larger amplitudes, which contribute predominantly to the probabilities, does not exceed 10 %. This translates to the TICS results calculated with the following field parameters: $\omega = 85$ eV, $T_1 = 6T$, $F_{\rm AC} = 0.1$ a.u. and $F_{\rm DC} = 0$. When overlaps are computed at the time of $T_1 = 6T$, $7T$ and $8T$, the resulting TICS values are 5.70 kb, 5.22 kb and 5.91 kb, respectively. Based on these figures, we adopt the value of 10% as a typical accuracy we can achieve in the present calculation.

IV. RESULTS.

A typical electrons energy distribution is shown in Figure 2 as a contour plot for the following field parameters: $\omega = 85$ eV, $T_1 = 6T$, $F_{\rm AC} = 0.1$ a.u. and $F_{\rm DC} = 0$. Here $F_{\rm AC}$ is the peak value of the AC field. Various shades of gray in the contour plot correspond to various magnitude of the function $P(E_1, E_2)$ as indicated on the right panel. Dashed line in the figure represents the energy conservation $E_1 + E_2 = E$, where $E = 6$ eV is the total excess energy for the given photon energy of 85 eV.

In Figure 3 we display results for TICS of DPI at photon energies of 85 and 90 eV and various applied DC field strengths. For both frequencies, the TICS exhibits decrease with the DC field. Such a behavior is not uncommon for two-electron systems in the external DC electric field when there are alternative routes of decay. For instance, it was observed for autoionizing states of helium for DC field strengths not exceeding certain critical values [33–35]. We documented recently a similar behavior of the total (single plus double) photoionization cross-section as a function of the external DC field for helium [36].

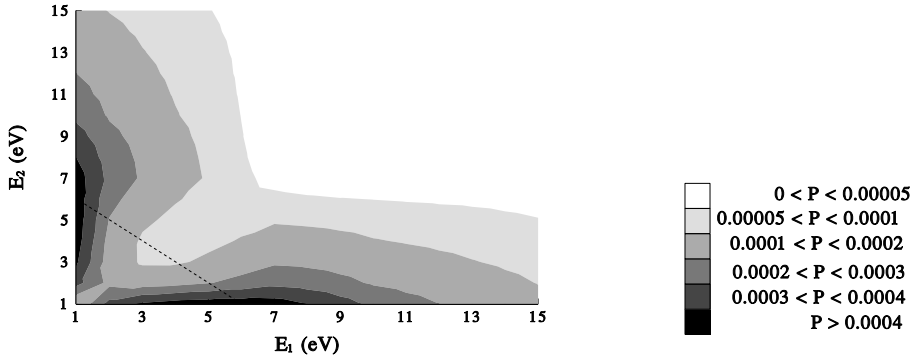

FIG. 2: Electron energy distribution $P(E_1, E_2)$ for the following field parameters: $\omega = 85$ eV, $T_1 = 6T$, $F_{\rm AC} = 0.1$ a.u., $F_{\rm DC} = 0$.

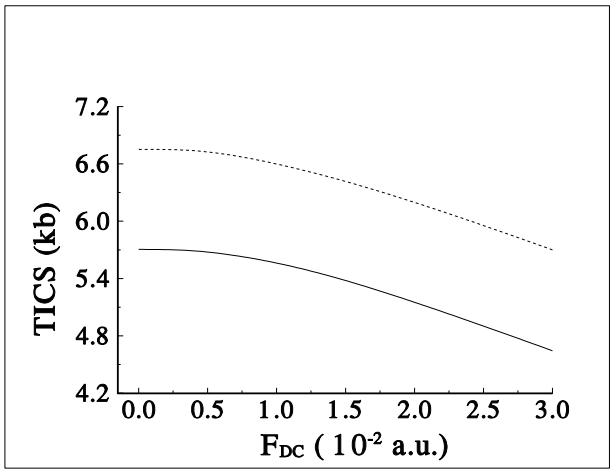

FIG. 3: Total integrated cross-section of DPI of helium as a function of an external DC field for photon energies of 85 eV (solid line) and 90 eV (dotted line)

More detailed picture of the effect of the external DC field on DPI can be obtained if we follow the evolution of the electron energy distribution function $P(E_1, E_2)$ with the strength of the DC field. This evolution is illustrated in Figure 4. For zero DC field, the energy distribution is shown in Figure 2.

Figure 4 shows monotonous decrease of the differential probability $P(E_1, E_2)$ in the (E_1, E_2)-plane. This decrease is not quite uniform. Rather pronounced feature visible in Figure 4 is a steady decrease of the probability to find both electrons with small energies

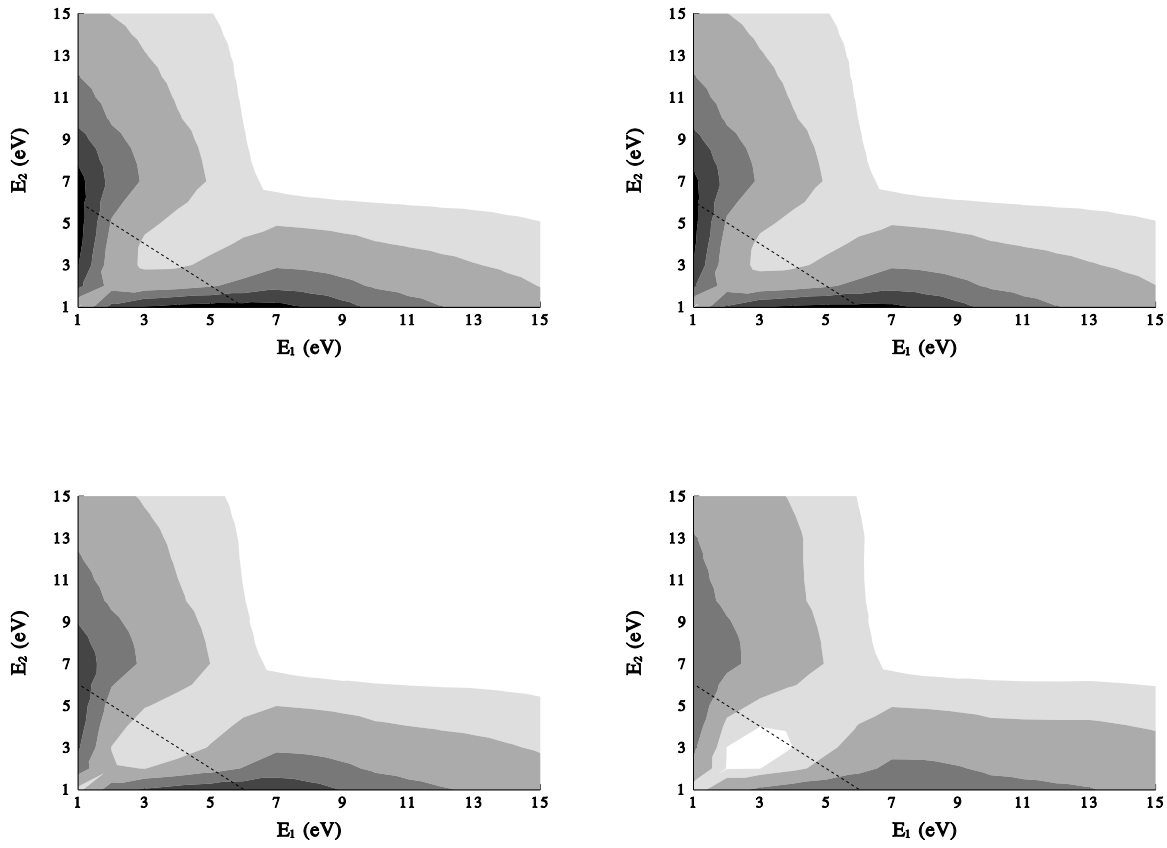

FIG. 4: Electron energy distribution $P(E_1, E_2)$ for $\omega = 85$ eV, $F_{\rm AC} = 0.1$ a.u. and $T_1 = 6T$. The DC field strength $F_{\rm DC}$ is 0.007, 0.01, 0.02, and 0.03 a.u. (from left to right and top to bottom). Various shades of grey have the same meaning as in Fig.2.

(white region near the origin). This reflects the fact that the DC field accelerates both electrons making it less probable to detect the electrons with small energies. Another noticeable characteristics is a rather rapid flattening of the surface $P(E_1, E_2)$ as a whole. This is probably a reflection of the fact that decay due to the presence of the DC field proceeds by tunneling. This process goes without energy conservation and may act, therefore, as an homogenizing agent, making the spectrum of outgoing electrons flat. This feature of the DC field can be more clearly noticed in Figure 5, where we plot the SDCS for various DC field strengths. The SDCS plot illustrates the behavior we outlined above. The decline of TICS occurs primarily due to the decline of the probability to detect electrons on the edges of the

distribution. We attribute this effect to the action of the DC field which tends to flatten the energy spectrum. We believe that this plot renders correctly the general features of the SDCS behavior with the DC field. The observed effect of the DC field on the SDCS is well above the quoted accuracy of 10%. The plot also shows small oscillations in the SDCS's which are probably just a reflection of the spurious time-dependence of the probabilities discussed above.

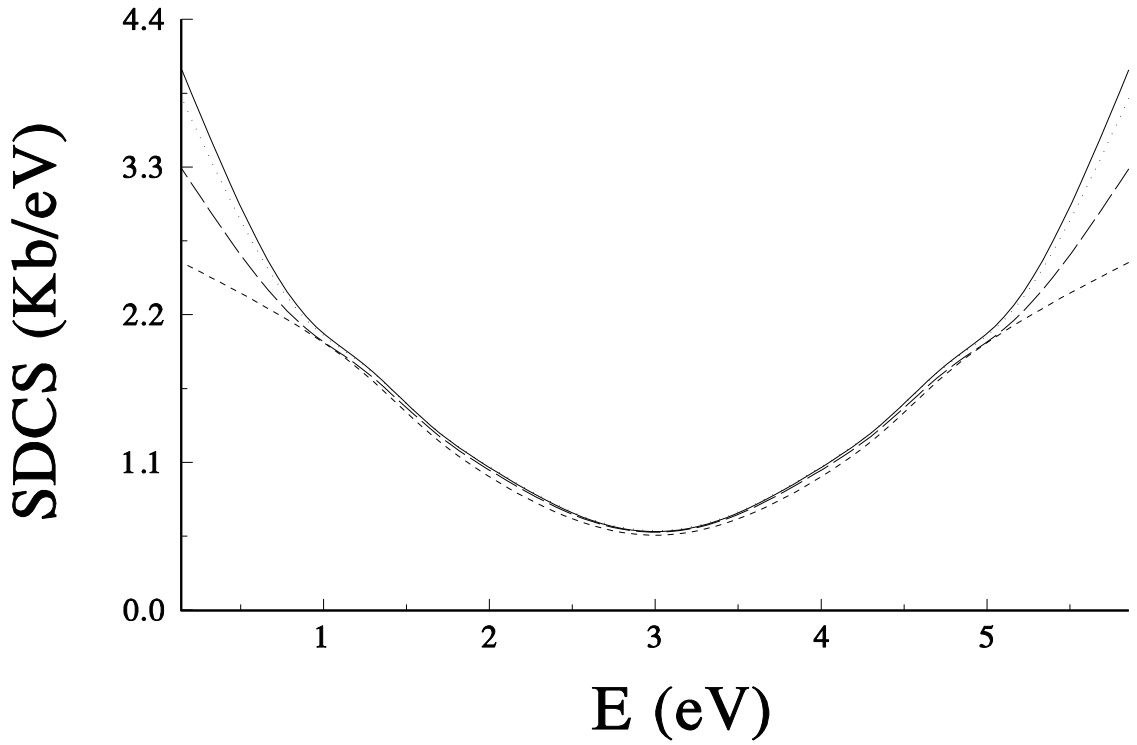

FIG. 5: Single differential cross section $d\sigma/dE$ of helium at various external DC field strengths. The AC field has the frequency $\omega = 85$ eV and the peak value $F_{\rm AC} = 0.1$ a.u. The DC field strength $F_{\rm DC}$ is zero (solid line), 1×10^{-2} a.u. (dots), 2×10^{-2} a.u. (long dash) and 3×10^{-2} a.u. (short dash).

As far as overall decline of TICS with the DC field is concerned, we have no such intuitive picture as in the case of SDCS. As we already mentioned in the Introduction, the double

ionization is a rather fragile balance between the inter-electron repulsion and the interaction with nucleus. If we adopt the classical view of the phenomenon, only a small fraction of the trajectories lead to the escape of both electrons. Our findings seem to indicate that external DC field changes the balance in favor of the trajectories leading to the one-electron escape.

V. CONCLUSION.

We have performed calculations of DPI of He for the photon frequencies of 85 and 90 eV in the presence of an external DC field. Our computational procedure is, in essence, a combination of the numerical integration of the TDSE in external AC and DC fields, and the CCC representation of the final field-free state.

We found that dependence of the TICS upon external DC field strength exhibits a monotonous decline. This decline occurs primarily due to the flattening of the energy spectrum of the outgoing electrons.

In the future, we intend to apply the combined TDSE-CCC technique to various time-dependent processes driven by short pulses of strong electromagnetic fields. In particular, we will study the two-photon double ionization of the helium atom and other targets subjected to radiation from a free-electron laser.

VI. ACKNOWLEDGEMENTS

The authors wish to thank Australian Partnership for Advanced Computing (APAC) for provision of their computing facilities. Support of the Australian Research Council in the form of Discovery grant DP0451211 is acknowledged.

---

[1] A. Huetz and J. Mazeau, Phys. Rev. Lett. **85**, 530 (2000).

[2] L. Spielberger, O. Jagutzki, R. Dorner, J. Ullrich, U. Meyer, V. Mergel, M. Unverzagt, M. Damrau, T. Vogt, I. Ali, et al., Phys. Rev. Lett. **74**, 4615 (1995).

[3] J. S. Briggs and V. Schmidt, J. Phys. B **33**, R1 (2000).

[4] G. C. King and L. Avaldi, J. Phys. B **33**, R215 (2000).

[5] L. Avaldi and A. Huetz, J. Phys. B **38**, S861 (2005).

[6] A. Becker, R. Dörner, and R. Moshammer, J. Phys. B **38**, S753 (2005).

[7] P. Bolognesi, L. Avaldi, I. Bray, R. Camilloni, M. Coreno, K. Kazansky, A. Kheifets, L. Malegat, P. Selles, G. Turri, et al., Physica Scripta **T110**, 104 (2004).

[8] P. Bolognesi, A. Kheifets, S. Otranto, M. Coreno, C. R. G. V. Feyer, F. Colavecchia, and L. Avaldi, J. Phys. B **39**, 1899 (2006).

[9] T. Weber, A. Czasch, O. Jagutzki, A. Müller, V. Mergel, A. Kheifets, E. Rothenberg, G. Meigs, M. Prior, S. Daveau, et al., Nature **431**, 437 (2004).

[10] W. Vanroose, F. Martin, T. N. Rescigno, and C. W. McCurdy, Science **310**, 1787 (2005).

[11] G. H. Wannier, Phys. Rev. **90**, 817 (1953).

[12] A. Scrinzi and B. Piraux, Phys. Rev. A **58**, 1310 (1998).

[13] J. Caillat, J. Zanghellini, M. Kitzler, O. Koch, W. Kreuzer, and A. Scrinzi, Phys. Rev. A **71**, 012712 (2005).

[14] I. F. Barna and J. M. Rost, Eur. Phys. J. D. **27**, 287 (2003).

[15] I. Bray, Phys. Rev. A **49**, 1066 (1994).

[16] C. W. McCurdy, T. N. Rescigno, and D. Byrum, Phys. Rev. A **56**, 1958 (1997).

[17] M. Baertschy, T. N. Rescigno, and C. W. McCurdy, Phys. Rev. A **64**, 022709 (2001).

[18] C. W. McCurdy, D. A. Horner, T. N. Rescigno, and F. Martin, Phys. Rev. A **69**, 032707 (2004).

[19] M. Pont and R. Shakeshaft, Phys. Rev. A **51**, 494 (1995).

[20] L. Malegat, P. Selles, and A. K. Kazansky, Phys. Rev. Lett. **85**, 4450 (2000).

[21] J. Colgan and M. S. Pindzola, Phys. Rev. Lett. **88**, 173002 (2002).

[22] J. Colgan and M. S. Pindzola, J. Phys. B **37**, 1153 (2004).

[23] I. Bray and A. T. Stelbovics, Adv. Atom. Mol. Phys. **35**, 209 (1995).

[24] S. Laulan and H. Bachau, Phys. Rev. A **68**, 013409 (2003).

[25] A. Becker and F. H. M. Faisal, J. Phys. B **38**, R1 (2005).

[26] J. R. Harries, J. P. Sullivan, J. B. Sternberg, S. Obara, T. Suzuki, P. Hammond, J. Bozek, N. Berrah, M. Halka, and Y. Azuma, Phys. Rev. Lett. **90**, 133002 (2003).

[27] X. M. Tong and C. D. Lin, Phys. Rev. Lett. **92**, 223003 (2004).

[28] C. Såthe, M. Ström, M. Agker, J. Soderstrom, J.-E. Rubensson, R. Richter, M. Alagia,

S. Stranges, T. W. Gorczyca, and F. Robicheaux, Phys. Rev. Lett. **96**, 043002 (pages 4) (2006).

[29] A. S. Kheifets and I. Bray, J. Phys. B **31**, L447 (1998).

[30] A. S. Kheifets and I. Bray, Phys. Rev. A **58**, 4501 (1998).

[31] K. Frankowski and C. L. Pekeris, Phys. Rev. **146**, 46 (1966).

[32] J. Colgan and M. S. Pindzola, Phys. Rev. A **65**, 032709 (2002).

[33] C. A. Nicolaides and S. I. Themelis, J. Phys. B **26**, L387 (1993).

[34] Y. K. Ho and J. Callaway, Phys. Rev. A **50**, 4941 (1994).

[35] I. A. Ivanov and Y. K. Ho, Phys. Rev. A **63**, 062503 (2001).

[36] I.A.Ivanov and A.S.Kheifets, Eur. Phys. J. D. **38**, 471 (2006).